DEHYDROCOUPLING OF $SiMe_2H$ SUBSTITUENTS IN PERMETHYLATED ZIRCONOCENE COMPLEXES

Jiří PINKAS[a1], Róbert GYEPES[b1,c], Ivana CÍSAŘOVÁ[b2], Jiří KUBIŠTA[a2], Karel MACH[a3] and Michal HORÁČEK[a4,*]

[a] *J. Heyrovský Institute of Physical Chemistry, Academy of Sciences of the Czech Republic, v.v.i., Dolejškova 3, 182 23 Prague 8, Czech Republic; e-mail: [1] pinkas@jh-inst.cas.cz, [2] kubista@jh-inst.cas.cz, [3] mach@jh-inst.cas.cz, [4] horacek@jh-inst.cas.cz*

[b] *Department of Inorganic Chemistry, Charles University, Hlavova 2030, 128 40 Prague 2, Czech Republic; e-mail: [1] gyepes@natur.cuni.cz, [2] cisarova@natur.cuni.cz*

[c] *Present address: J. Selye University, Pedagogical Faculty, Bratislavská cesta 3322, 945 01 Komárno, Slovak Republic,*

Received December 23, 2010
Accepted January 27, 2011
Published online February 15, 2011

Complex $[Zr\{\eta^5\text{-}C_5Me_4(SiMe_2H)\}_2Cl_2]$ (**1**) was prepared by the reaction of lithium salt of 2,3,4,5-tetramethyl-1-(dimethylsilyl)cyclopenta-2,4-diene with $[ZrCl_4]$ in boiling THF. The reduction of **1** with excess magnesium in THF in the presence of excess bis(trimethylsilyl)-acetylene (btmsa) afforded the bivalent metal *ansa*-disilylene complex with π-coordinated btmsa $[Zr(\eta^2\text{-btmsa})\{\eta^5\text{-}C_5Me_4(SiMe_2)\}_2]$ (**2**). The dehydrocoupling of $SiMe_2H$ groups was accompanied by a hydrogen transfer to releasing btmsa to give a mixture of *cis*- and *trans*-1,2-bis(trimethylsilyl)ethene. Chlorination of **2** with $PbCl_2$ afforded *ansa*-$[Zr\{\eta^5\text{-}C_5Me_4(SiMe_2)\}_2Cl_2]$ (**3**) and liberated btmsa. The crystal structures of complexes, **1**, **2** and **3** have been determined by X-ray crystallography.

Keywords: Metallocenes; Zirconium; Bridging ligands; Zirconocene; Dimethylhydrosilyl substituent; Dehydrocoupling; Bis(trimethylsilyl)acetylene complex; *ansa*-Zirconocene; Bis(dimethylsilylene) bridge; Crystal structure.

Early transition metal *ansa*-metallocene complexes are the subject of unceasing interest for about 30 years[1] because of their application as single-site catalysts for highly stereoregular polymerization of olefins[2]. Active catalytic species are generally obtained from *ansa*-metallocene dichloride precursors[3] either by activation with methylalumoxane or after their conversion to *ansa*-metallocene dialkyls by forming ionic pairs with tris-(pentafluorophenyl)borane[4]. The preparation of *ansa*-metallocene dichlorides has usually consisted of the synthesis of the *ansa*-dianionic ligand which was transmetallated with the metal tetrachloride $[MCl_4]$ (M = Ti, Zr,

© 2011 Institute of Organic Chemistry and Biochemistry
doi:10.1135/cccc2010155

Hf)[3a,3b,5a] except for the highly methyl-substituted titanocenes. These were reacted with $[TiCl_3 \cdot (THF)_3]$, and the obtained *ansa*-titanocene monochlorides[5b,5c] were oxidized with chlorinating agents like $PbCl_2$ or AgCl [6] to give the air-stable dichlorides. Yields of *ansa*-metallocene dichlorides are not generally high due to concurrent intermolecular transmetallation, and particularly for long *ansa*-bridging chains the yields are low[7]. The formation of the *ansa*-bridge from suitable substituents of cyclopentadienyl ligands in metallocene derivatives has been an alternative, usually highly selective and effective synthesis of *ansa*-metallocene compounds in special cases[8a]. Particularly useful were vinyl and ω-alkenyl substituents which afforded *ansa* compounds via photolysis[8b], catalyzed double bond metathesis with elimination of ethene[8c], or Mannich type coupling[8d,8e]. Removal of chlorine atoms by reducing agents resulted in coordination of pendant double bonds to metal divalent transient species and their subsequent coupling with the formation of ring-tethered metallacyclopentane complexes[9]. Following the latter concept of synthesis within the metallocene moiety, we have recently explored the use of the hydrodimethylsilyl substituent $SiMe_2H$ for the dehydrocoupling synthesis of *ansa*-bis(dimethylsilylene) bridge binding the titanocene tetramethylated cyclopentadienyl ligands. The subsequent oxidative chlorination with $PbCl_2$ then afforded *ansa*-$[TiCl_2\{\eta^5\text{-}C_5Me_4(SiMe_2)\}_2]$ in nearly quantitative yield[10].

Here we follow the above dehydrocoupling pathway for $[Zr\{\eta^5\text{-}C_5Me_4(SiMe_2H)\}_2Cl_2]$ (**1**) with the aim to prepare *ansa*-$[Zr\{\eta^5\text{-}C_5Me_4(SiMe_2)\}_2Cl_2]$ (**3**) and to characterize an intermediate zirconium(II) d^2 complex.

RESULTS AND DISCUSSION

The parent $[Zr\{\eta^5\text{-}C_5Me_4(SiMe_2H)\}_2Cl_2]$ complex was prepared by refluxing the $Li[C_5Me_4(SiMe_2H)]$ solution in THF with a half molar equivalent of $[ZrCl_4]$ until all solid zirconium chloride disappeared (Scheme 1). Pale yel-

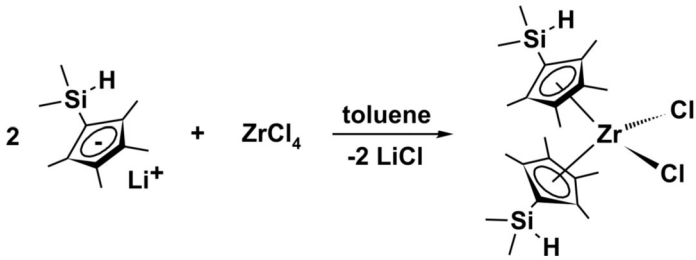

SCHEME 1

low crystalline **1** was obtained by extraction of the reaction residue with hexane in high yield.

The EI-MS spectra of **1** displayed a low-abundant molecular ion (*m/z* 518) and fragment ions after the loss of Me group or Cl atom. The spectra were further featured by a more abundant loss of the $SiMe_2H$ group, elimination of the whole cyclopentadienyl ligand giving rise to the base peak (*m/z* 339), and high-abundant ions $[SiMe_3]^+$ and $[SiMe_2H]^+$. The ^1H NMR spectrum gave evidence for the $SiMe_2H$ group showing the coupling between the methyl groups and the proton attached to the silicon atom ($^3J_{HH}$ = 3.9 Hz) giving rise to a doublet at 0.31 ppm for Si**Me**$_2$ and a septuplet at 4.74 ppm for Si**H**. The resonance of methyl groups in proximal position to the $SiMe_2H$ substituent (denoted α) is downfield shifted with respect to those in distal positions (denoted β) as evidenced from irradiation of $SiMe_2$ group in 1D NOESY experiment. The Si–H bond was also clearly identified in IR spectrum giving rise to a very strong absorption band at 2149 cm^{-1}. Strong intensity absorption bands at 1251 and 1246 cm^{-1} and very strong bands at 877 and 839 cm^{-1} are typical for the Si–Me species, being virtually unified for the $SiMe_3$ group, e.g. in $[Zr(\eta^5\text{-}C_5Me_4SiMe_3)_2Cl_2]$ [11] or $[Ti(\eta^5\text{-}C_5Me_4\text{-}SiMe_3)_2Cl_2]$ [12]. The molecular structure of **1** was determined by X-ray single crystal diffraction analysis (see below).

Compound **1** was reduced with an excess of magnesium in THF in the presence of a three-fold molar excess of bis(trimethylsilyl)acetylene (btmsa) to give the green Zr(II) zirconocene–btmsa complex *ansa*-$[Zr(\eta^2\text{-btmsa})\text{-}\{\eta^5\text{-}C_5Me_4(SiMe_2)\}_2]$ (**2**) containing the bis(dimethylsilylene) bridge between the cyclopentadienyl ligands (Scheme 2).

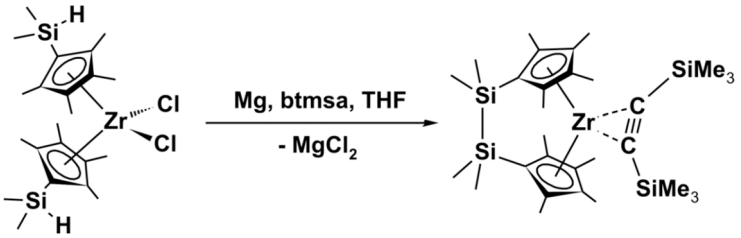

Scheme 2

The absence of Si–H bonds and the presence of the π-bonded btmsa in **2** was proved by EI-MS, IR, and ^1H, ^{13}C and ^{29}Si NMR spectra whereas the presence of the *ansa*-$SiMe_2SiMe_2$ bridge was unequivocally proved by the crystal structure (see below). The EI-MS spectra showed the molecular ion of very low abundance and a highly abundant *ansa*-zirconocene ion after

elimination of btmsa. The btmsa elimination was largely thermally-induced[13] as evidenced by decreasing intensity of ions $[btmsa]^{\bullet+}$ and $[btmsa - Me]^+$ during the spectra scanning. The base peak $[SiMe_3]^+$ and abundant peak of $[SiMe_2H]^+$ arose from fragmentation of the *ansa*-zirconocene as they keep constant relative to the parent ion. In IR spectra, the ν(Si–H) absorption band was absent and new medium-intensity absorption bands at 1549 and 1523 cm^{-1} were assigned to the stretching C≡C vibration of the coordinated btmsa, their average value being shifted by 570 cm^{-1} from the value for free btmsa[14]. The presence of more absorption bands for the ν(C≡C) vibrations were usually observed for various cyclopentadienyl-substituted titanocene–btmsa complexes[15]. ^{1}H NMR spectra proved the absence of the Si**H** resonance, the singularity of the Si**Me**$_2$ signal, equal integral intensities for $SiMe_2$, α-Me and β-Me protons and opposite shifts for α- and β-methyl groups of the cyclopentadienyl ligands. The observed down-field shift of β-methyl group resonance apparently results from anisotropic deshielding of the distal methyl groups by btmsa triple bond. This suggestion was corroborated by 1D NOESY experiments showing a strong through-space interaction between protons of β-Me and $SiMe_3$ of the coordinated btmsa. The distal methyl groups were also found in vicinity of the coordinated triple bond in the crystal structure of **2** (see below). The most typical feature of ^{13}C NMR spectra of **2** is a high downfield shift of quaternary carbons of btmsa to 259.3 ppm. This is a common property of btmsa back-bonded to metallocenes (M^{II}) of early transition metals[15,16] whose another expression is the elongation of the triple bond corresponding roughly to a decrease of one bonding order (see below). The presence of back-bonded btmsa was also confirmed by electronic absorption band at 733 nm which is typical for $[Zr(\eta^2\text{-btmsa})Cp'_2]$ ($Cp' = C_5H_{5-n}Me_n$, n = 5–3) complexes[17]. This band has been assigned to $b_2 \rightarrow 1a_1$ transition on the basis of DFT calculations carried out for $[Ti(\eta^2\text{-btmsa})Cp)_2]$ [19]. The most important spectroscopic data which could correlate with the strength of btmsa coordination in **2** and some highly methyl-substituted zirconocene–btmsa complexes are gathered in Table I. Inspection of the data leads to a conclusion that the different methods afford different orders, and that within one method at least one value is rather unexpected. Another drawback is a limited precision of the data, particularly those for ν(C≡C). The latter value should be taken as a center of gravity for integrated absorption bands related to this vibration(s). This is, however, impossible for the complexes possessing the strongly bonded btmsa absorbing below 1500 cm^{-1} because this range is dominated by C–H deformation vibrations. Based on the ν(C≡C) wavenumber data which should correlate with the crystallographic C–C bond length (d(C–C),

Table I) it can be assumed that btmsa in **2** is bound weaker than in [Zr(η^2-btmsa){η^5-C_5Me_5}$_2$] which is taken as a reference.

The air-stable compound *ansa*-[Zr{η^5-$C_5Me_4(SiMe_2)$}$_2Cl_2$] (**3**) was prepared from **2** by oxidative chlorination with $PbCl_2$ in THF according to Scheme 3.

TABLE I
NMR (δ, ppm), IR (ν, cm^{-1}), UV-Vis (λ, nm) and crystallographic (*d*, Å) data for η^2-btmsa in [Zr(η^2-btmsa)Cp′$_2$] complexes

Cp′	$^1H(SiMe_3)$	$^{13}C(SiMe_3)^a$	$^{13}C(C{\equiv}C)^a$	$\nu(C{\equiv}C)^b$	λ	d(C–C)	Ref.
$C_5Me_4SiMe_2$	0.17	4.2	259.3	1549	733	1.311(7)	This work
$C_5Me_4SiMe_3$	0.16, 0.20[c]	2.8, 4.9[c]	259.5	1500	740	1.327(5)	11
C_5Me_5	0.20	4.0	260.5	1516	725	1.320(3)	17
C_5Me_4H	0.14	3.4	260.2	1516	738	1.316(3)	17
$C_5Me_3H_2$	0.14	2.8	260.0	1535	745	–	17
C_5Me_4Ph	0.13	3.7	259.8	1515	727	1.333(5)	18

[a] Chemical shifts for noncoordinated btmsa (C_6D_6, 23 °C): ^{13}C(Me) δ 0.2 q, $^{13}C(C{\equiv}C)$ δ 113.8 s (ref.[14]). [b] The band of the highest wavenumber in the relevant region. [c] For $SiMe_3$ on either cyclopentadienyl or btmsa ligand

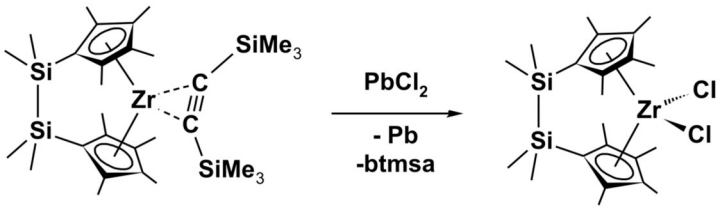

SCHEME 3

The liberated btmsa was identified by GC-MS and identity of **3** was proved by spectroscopic methods and elemental analysis. An increase in the stability of **3** compared to **1** was demonstrated by EI-MS spectra showing the molecular ion as a base peak. The ^1H NMR spectrum revealed the same 1:1:1 integral ratio of $SiMe_2$, α-Me and β-Me protons as for **2**, and a similar downfield shift of β-Me with regard to α-Me protons. The difference between the chemical shifts for β-Me and α-Me protons is somewhat reduced due to a lower deshielding effect of σ-Ti–Cl bond compared to a strong deshielding induced by the triple bond in **2**. The molecular structure of **3** was established by X-ray single crystal diffraction analysis.

*Crystal Structures of **1–3***

PLATON drawings of molecular structures of **1–3** are shown in Figs 1–3, respectively, and common geometric parameters are listed in Table II.

The dichlorides **1** and **3** crystallized in the monoclinic space group *C2/c* (No. 15) and their molecules were symmetrical with respect to the crystallographic two-fold axis, passing through the zirconium atom and the centre of the line defined by the two chlorine atoms. In **1**, the sterically demanding $SiMe_2H$ groups are orientated in lateral positions with respect to the

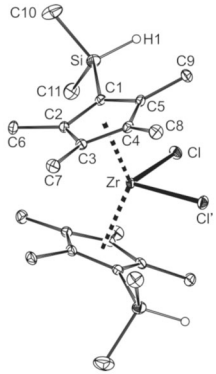

FIG. 1
PLATON drawing of compound **1** at the 30% probability level, with atom labeling scheme. Hydrogen atoms except H(1) on the silicon atoms are omitted for clarity

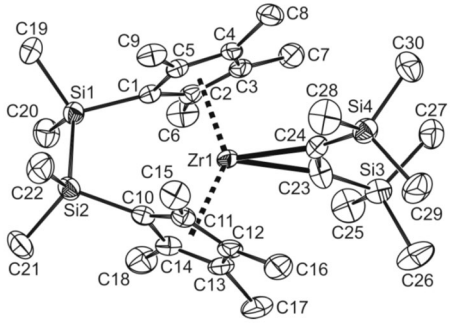

FIG. 2
PLATON drawing of compound **2** at the 30% probability level, with atom labeling scheme. Hydrogen atoms are omitted for clarity

TABLE II
Selected bond lengths (in Å) and angles (in °) for compounds **1–3**

	1[a]	**2**	**3**[a]
Bond lengths			
Zr–Cg(1)[b]	2.2442(11)	2.242(2)	2.2431(9)
Zr–Cg(2)[b]	–	2.252(2)	–
Zr–P1(1)[b]	2.2413(1)	2.240(1)	2.2400(1)
Zr–P1(2)[b]	–	2.251(1)	–
Zr–Cl	2.4476(6)	2.274(5)[c]	2.4371(6)
Zr–C(24)	–	2.2911(4)	–
Si(1)–Si(2)	–	2.348(2)	2.3415(12)
Bond and dihedral angles			
Cl–Zr–Cl′	91.31(3)	–	96.16(3)
Cg(1)–Zr–Cg(2)	136.74(4)	137.89(8)	136.12(3)
φ[d]	41.30(8)	45.82(15)	49.98(6)
τ[e]	–	18.65(8)	16.03(8)

[a] Symmetry transformation used to generate equivalent atoms: $1 - x, y, -z + 1/2$. [b] Cg(1) and Cg(2) are centroids and Pl(1) and Pl(2) least-square planes of the C(1–5) and C(11–15) cyclopentadienyl rings, respectively. [c] The bond length for Zr–C(23). [d] Dihedral angle between the Pl(1) and Pl(2) planes. [e] Dihedral angle between the Si(1), Zr, Si(2) and Cg(1), Zr, Cg(2) planes; for **1** and **3** read symmetry equivalent Si′ and Cg′ positions.

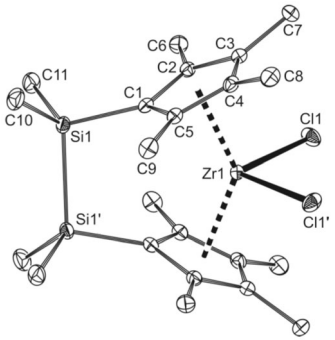

FIG. 3
PLATON drawing of compound **3** at the 30% probability level, with atom labeling scheme. Hydrogen atoms are omitted for clarity

crystallographic twofold axis, and their Si–H bonds (1.39(2) Å) are directed towards the zirconocene open shell, to the side of the chlorine atoms (Fig. 1). The linking of silicon atoms in **3**, somewhat surprisingly, did not affect the Zr–Cg and Zr–Pl(1) distances and only slightly decreased the Cg–Zr–Cg angle. On the other hand, the angle between the least-squares planes of the cyclopentadienyl rings (φ) was increased by more than 8°, and this induced an increase in the Cl–Zr–Cl angle by about 5° (see Table II). The crystallographically asymmetrical molecule of **2** contains the back-bonded btmsa ligand whose bent structure mimicking the sp^2 hybridization on the acetylenic carbon atoms is very common for all known early transition metal (Ti, Zr and Hf) metallocene complexes[15–17]. Compound **2** differs only negligibly from **3** in zirconocene geometry parameters except for a lower magnitude of angle φ (45.82(15) vs 49.98(6)°). This can indicate that the btmsa ligand imposes a lower steric demand than the two chlorine atoms in **3**, however, different metal bonding orbital schemes for σ-bonding in **3** and back-bonding in **2** can play a role. The C–C bond length of 1.312(7) Å for the back-bonded btmsa ligand in **2** is the shortest of the distances listed for $[Zr(\eta^2\text{-btmsa})Cp'_2]$ complexes in Table I that should imply the weakest bonding of the ligand. This is in rough agreement with the highest value of its ν(C≡C) wavenumber, however at partial variance with other spectral data in Table I.

Compared to analogous titanium complexes (for crystal structure of *ansa*-$[Ti\{\eta^5\text{-}C_5Me_4(SiMe_2)\}_2Cl_2]$ see ref.[20]) complexes **1–3** are crystallographically isomorphous, the main difference in geometric parameters being caused by a larger covalent radius of Zr atom. As a result larger volumes of unit cell (by 24–69 $Å^3$), longer M–Cg and M–C bond lengths (by > 0.1 Å) or M–Cl bond lengths (by < 0.1 Å) were found for the zirconium compounds. A smaller elongation of the polar Zr–Cl bond apparently reflects a lower electronegativity of Zr with respect to Ti (nominal 1.4 vs 1.5).

On the Dehydrocoupling Mechanism

The reduction-induced dehydrocoupling summarized in Scheme 2 has to involve the reduction of Zr(IV) to Zr(II) valence state which is commonly stabilized by coordination of btmsa in a π-mode back-bonding. This reduction step is generally more difficult for zirconium than for titanium since the first standard reduction potential of various zirconocene dichlorides is by about 1.0 V higher than for the corresponding titanocene dichlorides. Moreover, the methyl substituents on the Cp′ ligands further increase this potential with an increment of –71 mV per one Me group[21]. On the other

hand, the btmsa ligand is more strongly bonded in zirconium complexes than in titanium ones as evidenced by a larger down-field shift of δ_C for the coordinating carbon atoms (by ca. 11 ppm) and a larger shift of $\nu(C{\equiv}C)$ to lower wavenumber (by ca. 50 cm^{-1}). Surprisingly, the coordinated triple bond in **2** (1.311(3) Å) is virtually not elongated with respect to that of the titanium analogue (1.309(3) Å)[10]. The stronger bonding of btmsa is probably a reason for much lower effectivity of catalysis of linear dimerization of terminal alkynes to head-to-tail dimers for zirconocene–btmsa complexes[22] compared to titanocene–btmsa ones[23].

The dehydrocoupling step is believed to be preceded by agostic interaction of Si–H bonds to the zirconium atom. This is followed by the hydrogen transfer to the coordinated btmsa ligand and the formation of Si–Si bond. The metal–hydrogen agostic bonding[24] was so far proved in complexes where the Si–H bond was situated in the open shell of the bent metallocene, as in the zirconium d^0 complex $[ZrCl(\eta^5\text{-}C_5H_5)_2N(t\text{-}Bu)SiMe_2H]$ with the $SiMe_2H$ group attached to zirconium[25] or in the d^2 complexes $[M(\eta^5\text{-}C_5H_5)_2(\eta^2\text{-}(t\text{-}Bu)C{\equiv}CSiMe_2H)]$ (M = Ti, Zr and Hf)[26]. In the present case, the agostic intermediate was not entrapped as the intramolecular hydrogen transfer likely proceeds with low activation energy. The products of the hydrogen transfer, 1,2-bis(trimethylsilyl)ethenes (trans >> cis) can not bind to the formed *ansa*-zirconocene mainly due to steric hindrance between the π-coordinated substituted olefin and zirconocene cyclopentadienyl shell. In the presence of excessive btmsa, the olefin is completely replaced with the alkyne, as established for **2**.

EXPERIMENTAL

General

All manipulations including spectroscopic measurements were performed under high vacuum using all-sealed glass devices equipped with breakable seals or carried out under argon atmosphere (organic ligands). ^1H, ^{13}C $\{^1H\}$ and ^{29}Si $\{^1H\}$ (INEPT technique) NMR spectra were recorded on a Varian Mercury 300 spectrometer at 300, 75.4 and 59.6 MHz, respectively, in C_6D_6 solutions at 25 °C. Coupling constants (*J*) are given in Hz. Chemical shifts (δ, ppm) are reported relative to the residual solvent signal (δ_H 7.15) and to the solvent resonance (δ_C 128.00). The δ_{Si} values are related to tetramethylsilane as external standard. The standard NMR techniques as APT, 1D NOESY, gCOSY, gHMQC and gHMBC were used for detailed assignments of the signals. Methyl groups on cyclopentadienyl ring are labeled α and β for the proximal or distal position with respect to the silyl substituent, respectively. EI-MS spectra were obtained on a VG-7070E double-focusing mass spectrometer at 70 eV. Crystalline samples in sealed capillaries were opened and inserted into the direct inlet under argon. The spectra are represented by the peaks of relative abundance higher than 7% and by important peaks of lower intensity. Crystals for EI-MS measurements, melting point de-

termination, and for X-ray analysis were placed in glass capillaries in a Labmaster 130 glovebox under purified nitrogen (mBraun, O_2 and H_2O concentrations lower than 1.0 ppm) which were temporarily closed with a wax and then sealed with a flame. KBr pellets were prepared in the glovebox and measured in an air-protecting cuvette on a Nicolet Avatar FTIR spectrometer in the range of 400–4000 cm^{-1}. Elemental analyses were carried out on a FlashEA 2000 CHN/O Automatic Elemental Analyzer (Thermo Scientific). GC-MS measurements were performed on a Thermo Focus DSQ using the capillary column Thermo TR-5MS (15 m × 0.25 mm ID × 0.25 μm). UV-Vis measurements were performed using an all-sealed glass device with attached quartz cuvettes (Hellma) on a Varian Cary 17D spectrometer in the 300–2000 nm range.

Chemicals

The solvents tetrahydrofuran (THF), hexane, toluene and benzene-d_6 were purified by conventional methods, dried by refluxing over $LiAlH_4$, and stored as solutions of dimeric titanocene $[(\mu\text{-}\eta^5\text{:}\eta^5\text{-}C_{10}H_8)\{(\eta^5\text{-}C_5H_5)Ti(\mu\text{-}H)\}_2]$ [27]. Bis(trimethylsilyl)acetylene (Aldrich) was degassed, stored as a solution of green dimeric titanocene for 4 h, and distilled into ampules. Magnesium turnings (purum for Grignard reactions) and $PbCl_2$ (Aldrich) were weighed and evacuated. Me_2SiHCl and $[ZrCl_4]$ (both Aldrich) were handled under nitrogen atmosphere. 1.6 M Butyllithium (BuLi) in hexane and $LiAlH_4$ (both Aldrich) were used under argon as received. 5-(Dimethylsilyl)-1,2,3,4-tetramethylcyclopenta-1,3-diene was prepared as reported[10].

Preparation of $[Zr\{\eta^5\text{-}C_5Me_4(SiMe_2H)\}_2Cl_2]$ (**1**)

5-(Dimethylsilyl)-1,2,3,4-tetramethylcyclopenta-1,3-diene (7.2 g, 40.0 mmol) was diluted with 250 ml of diethyl ether, cooled to 0 °C, and 1.6 M BuLi in hexane (25.0 ml, 40.0 mmol) was added under stirring. After stirring for 1 h, a white precipitate of the cyclopentadienyllithium salt was separated, washed with 50 ml of diethyl ether and dried under vacuum. This was dissolved in 100 ml of THF, and the solution added to a suspension of $ZrCl_4$ (4.62 g, 20 mmol) in 20 ml of THF. The mixture was stirred and refluxed for 40 h. Then all volatiles were removed in vacuum, and an oily residue was extracted with hexane. A pale yellow solution was concentrated and cooled to –18 °C. Pale yellow crystals of **1** were separated and dried in vacuum. Yield 8.3 g (80%). M.p. 148 °C. ^{1}H NMR (C_6D_6): 0.31 (d, $^3J_{HH}$ = 3.9, 12 H, Si**Me**$_2$H); 1.81 (s, 12 H, C_5Me_4, β-Me); 2.18 (s, 12 H, C_5Me_4, α-Me); 4.74 (septuplet, $^3J_{HH}$ = 3.9, 2 H, $SiMe_2$**H**). ^{13}C {^{1}H} NMR (C_6D_6): –2.11 (Si**Me**$_2$H); 12.12, 15.20 (C_5**Me**$_4$); 118.15 (C_{ipso}); 128.13, 133.49 (C_q, **C**$_5$Me$_4$). ^{29}Si {^{1}H} NMR (C_6D_6): –26.40 ($SiMe_2H$). EI-MS (direct inlet, 70 eV, 160 °C), *m/z* (rel. abundance): 520 (8), 519 (6), 518 ($M^{\bullet+}$; 7), 507 (6), 505 (8), 504 (4), 503 ([M – Me]$^+$; 7), 483 ([M – Cl]$^+$; 5), 465 (7), 463 (15), 462 (8), 461 (20), 460 (9), 459 ([M – $SiMe_2H$]$^+$; 20), 347 (13), 346 (9), 345 (54), 344 (24), 343 (97), 342 (54), 341 (100), 340 (70), 339 ([M – $C_5Me_4SiMe_2H$]$^+$; 99), 338 (11), 337 (26), 301 (8), 299 (9), 289 (7), 287 (12), 286 (7), 285 (16), 247 (6), 245 (11), 243 (9), 241 (9), 180 (13), 179 ([$C_5Me_4SiMe_2H$]$^+$; 14), 178 (8), 163 (9), 149 (8), 119 (24), 105 (11), 97 (8), 73 ([$SiMe_3$]$^+$; 25), 59 ([$SiMe_2H$]$^+$; 73). IR (KBr, cm^{-1}): 2955 (s), 2912 (s), 2149 (vs), 1537 (w), 1483 (m), 1440 (m), 1380 (m), 1358 (w), 1336 (s), 1251 (s), 1246 (s), 1153 (w), 1128 (m), 1022 (m), 995 (w), 956 (w), 877 (vs), 839 (vs), 823 (m), 765 (s), 746 (w), 729 (m), 701 (w), 656 (m), 641 (w), 627 (w), 579 (w), 551 (w), 536 (w), 423 (m). For $C_{22}H_{38}Cl_2Si_2Zr$ (520.85) calculated: 50.73% C, 7.35% H; found: 50.69% C, 7.32% H.

TABLE III
Crystallographic data and details of the data collection and structure refinement for **1–3**

	1	**2**	**3**
Formula unit	$C_{22}H_{38}Cl_2Si_2Zr$	$C_{30}H_{54}Si_4Zr$	$C_{22}H_{36}Cl_2Si_2Zr$
M	520.82	618.31	518.81
Crystal system	monoclinic	triclinic	monoclinic
Space group	*C*2/*c* (No. 15)	*P-1* (No. 2)	*C*2/*c* (No. 15)
a (Å)	18.4869(11)	9.3250(4)	15.0216(5)
b (Å)	8.1784(3)	11.8090(4)	9.6130(3)
c (Å)	16.6874(10)	16.9400(7)	17.6774(5)
α (deg)	90.00	94.431(3)	90.00
β (deg)	95.092(2)	104.773(2)	107.946(2)
γ (deg)	90.00	104.676(2)	90.00
V (Å^3); *Z*	2513.1(2); 4	1724.72(12); 2	2428.47(13); 4
D_{calcd} (g cm^{-3})	1.377	1.191	1.419
μ (mm^{-1})	0.752	0.474	0.778
Color; habit	yellow; block	green; fragment	yellow; prism
Crystal size (mm^3)	0.75 × 0.12 × 0.08	0.50 × 0.40 × 0.20	0.35 × 0.28 × 0.25
T (K)	150(2)	293(2)	150.0(1)
θ_{min}; θ_{max} (deg)	1.00; 27.48	1.00; 25.00	2.63; 27.49
Range of *h*	–23→23	–11→10	–19→19
Range of *k*	–10→9	–14→14	–12→12
Range of *l*	–21→21	–20→20	–22→22
Diffractions collected	7745	16471	17988
Diffractions unique	2862	5985	2795
F(000)	1088	660	1080
Number of parameters	133	334	129
$R(F)$; $R_w(F^2)$ all data %	5.09; 7.14	6.32; 13.82	4.08; 7.60
GOF (F^2), all data	1.033	1.114	1.052
$R(F)$; $R_w(F^2)$ ($I > 2\sigma(I)$)	3.44; 6.51	5.03; 12.92	3.08; 7.10
Δρ (e Å^{-3})	0.389; –0.478	0.589; –0.581	0.548; –0.586

Preparation of $[Zr\{\eta^2\text{-}Me_3SiC{\equiv}CSiMe_3\}\{Me_4Si_2(\eta^5\text{-}C_5Me_4)_2\}]$ (**2**)

Compound **1** (2.07 g, 4.0 mmol) was mixed with excess of Mg (0.2 g, 8 mmol) and btmsa (2.2 ml, 10 mmol) in THF (50 ml), and the mixture was heated to 60 °C until its color turned from dark yellow to dark green (5 days). All volatiles were evaporated in vacuum at 60 °C, and the residue was extracted with hexane. After cooling to –18 °C, the concentrated dark green solution afforded green crystals of **2**. Yield 1.6 g (65 %). ^{1}H NMR (C_6D_6): 0.17 (s, 18 H, $SiMe_3$); 0.36 (s, 12 H, $SiMe_2$); 1.51 (s, 12 H, α-Me); 2.22 (s, 12 H, β-Me). ^{13}C {^{1}H} NMR (C_6D_6): 0.40 ($SiMe_2$); 4.24 ($SiMe_3$); 13.25, 13.46 ($C_5\mathbf{Me}_4$); 112.78 ($\mathbf{C}_{ipso}$, $\mathbf{C}_5Me_4$); 124.96, 127.07 ($\mathbf{C}_5Me_4$); 259.33 ($\mathbf{C}SiMe_3$). ^{29}Si {^{1}H} NMR (C_6D_6): –19.58, –15.03 ($SiMe_3$ and $SiMe_2$). EI-MS (direct inlet, 70 eV, 160 °C), *m/z* (rel. abundance): 616 ($M^{\bullet+}$; 1), 452 (9), 450 (24), 449 (13), 448 (33), 447 (36), 446 ([M – btmsa]$^+$; 60), 238 (8), 237 ([$C_5Me_4SiMe_2SiMe_2H$]$^+$; 28), 179 ([$C_5Me_4SiMe_2H$]$^+$; 7), 174 (13), 170 ([btmsa]$^+$; 4), 155 ([btmsa-Me]$^+$; 21), 131 (11), 117 (12), 87 (11), 86 (25), 85 (19), 74 (17), 73 ([$SiMe_3$]$^+$; 100), 59 ([$SiMe_2H$]$^+$; 58). IR (KBr, cm^{-1}): 2950 (s), 2899 (s), 1549 (w), 1523 (w), 1482 (w), 1453 (w), 1408 (w), 1380 (w), 1355 (w), 1333 (m), 1245 (vs), 1131 (w), 1082 (w), 1021 (w), 962 (w), 839 (vs), 830 (vs), 811 (s), 788 (s), 759 (m), 725 (w), 683 (w), 671 (m), 654 (m), 620 (w), 570 (w), 465 (m), 447 (w), 420 (w). UV-Vis (toluene, nm): 318 > 361 (sh) >> 733. For $C_{30}H_{54}Si_4Zr$ (618.33) calculated: 58.27% C, 8.80% H; found: 58.32% C, 8.84% H.

Preparation of $[Zr\{Me_4Si_2(\eta^5\text{-}C_5Me_4)_2\}Cl_2]$ (**3**)

Compound **2** (1.23 g, 2.0 mmol) was dissolved in 50 ml of THF, and $PbCl_2$ (0.55 g, 2.0 mmol) was added. The mixture was stirred at 60 °C while its color was changing from green to yellow. After 2 h, the solvent and all volatiles were distilled in vacuum into a trap cooled with liquid nitrogen, finally at 60 °C. A dry yellow residue was exhaustively extracted with hexane. Cooling of the hexane solution to –18 °C afforded a yellow crystalline solid. Its recrystallization from toluene afforded yellow crystals of **3**. Yield 0.77 g (74%). ^{1}H NMR (C_6D_6): 0.36 (s, 12 H, $SiMe_2$); 1.91 (s, 12 H, α-Me); 2.07 (s, 12 H, β-Me). ^{13}C {^{1}H} NMR (C_6D_6): 0.19 ($SiMe_2$); 13.03, 15.30 ($C_5\mathbf{Me}_4$); 124.76, 125.60, 135.26 ($\mathbf{C}_5Me_4$). ^{29}Si {^{1}H} NMR (C_6D_6): –13.92 ($SiMe_2$). EI-MS (direct inlet, 70 eV, 130 °C), *m/z* (rel. abundance): 522 (10), 521 (14), 520 (55), 519 (51), 518 (100), 517 (51), 516 ($M^{\bullet+}$; 94), 504 (9), 503 (12), 502 (6), 501 ([M – Me]$^+$; 12), 467 (5), 465 ([M – Me – HCl]$^+$; 7), 458 (6), 457 ([M – $SiMe_2H$]$^+$; 13), 443 ([M – $SiMe_3$]$^+$; 6), 429 (14), 428 (6), 427 (28), 426 (12), 425 (42), 424 (18), 423 ([M – $SiMe_2Cl$]$^+$; 33), 421 (7), 342 (10), 340 (18), 338 ([M – $C_5Me_4SiMe_2$]$^+$; 13), 325 (11), 323 (16), 299 (10), 289 (11), 287 (15), 286 (9), 285 (20), 178 (20), 177 (39), 147 (11), 120 (8), 119 (40), 105 (14), 97 (19), 93 (11), 83 (15), 73 ([$SiMe_3$]$^+$; 42), 59 ([$SiMe_2H$]$^+$; 76), 58 (12). IR (KBr, cm^{-1}): 2979 (s), 2947 (s), 2911 (s), 1453 (m), 1405 (w), 1379 (s), 1354 (w), 1331 (s), 1256 (s), 1246 (m), 1153 (w), 1129 (w), 1021 (s), 856 (m), 829 (vs), 815 (s), 795 (s), 767 (m), 745 (w), 733 (w), 692 (w), 676 (s), 658 (s), 466 (m), 436 (s). For $C_{22}H_{36}Cl_2Si_2Zr$ (518.83) calculated: 50.93% C, 7.00% H; found: 50.86% C, 6.96% H.

The volume of collected volatiles from the reaction was reduced at normal pressure to ca. 20%. GC-MS analysis of the residue revealed besides THF free btmsa and traces of unidentified compounds at longer retention times.

X-ray Structure Determination

Crystal fragments of **1–3** were fixed into Lindemann glass capillaries under nitrogen in a glovebox and were sealed with wax. Diffraction data were collected on a Nonius KappaCCD diffractometer and processed by the HKL program package[28]. The structures were solved by direct methods (SIR92)[29] and refined by full-matrix least-squares on F^2 (SHELXL97)[30]. All non-hydrogen atoms were refined anisotropically. The hydrogen atoms residing on the silicon atoms for **1** were refined without any constraints while all other hydrogen atoms were included in ideal positions. Relevant crystallographic data for all the compounds are given in Table III. Molecular graphics were done with (PLATON)[31]. CCDC 804294 (for **1**), 805527 (for **2**) and 804295 (for **3**) contain the supplementary crystallographic data for this paper. These data can be obtained free of charge via www.ccdc.cam.ac.uk/conts/retrieving.html (or from the Cambridge Crystallographic Data Centre, 12, Union Road, Cambridge, CB2 1EZ, UK; fax: +44 1223 336033; or deposit@ccdc.cam.ac.uk).

This research was supported by the Grant Agency of the Academy of Sciences of the Czech Republic (Grant No. IAA400400708) and the Ministry of Education, Youth and Sports of the Czech Republic (Project No. LC06070). I.C. is grateful to MSM0021620857. The authors are also grateful to Ms D. Kapková for excellent glassblowing assistance.

REFERENCES

1. Smith J. A., von Seyerl J., Huttner G., Brintzinger H. H.: *J. Organomet. Chem.* **1979**, *173*, 175.
2. a) Kaminsky W., Külper K., Brintzinger H. H., Wild F. R. W. P.: *Angew. Chem., Int. Ed. Engl.* **1985**, *24*, 507; b) Brintzinger H. H., Fischer D., Mülhaupt R., Rieger B., Waymouth R. M.: *Angew. Chem., Int. Ed. Engl.* **1995**, *34*, 1143; c) Janiak C. in: *Metallocenes* (A. Togni and Halterman R. L., Eds), Vol. 2, pp. 547–623. Wiley-VCH, Weinheim 1998; d) Gladysz J. A. (Ed.): *Frontiers in Metal-Catalyzed Polymerization. Chem. Rev.* **2000**, *100*, 167-1604; e) Alt H. G., Licht E. H., Licht A. I., Schneider K. J.: *Coord. Chem. Rev.* **2006**, *250*, 2; f) Möhring P. C., Coville N. J.: *Coord. Chem. Rev.* **2006**, *250*, 18; g) Razavi A., Thewalt U.: *Coord. Chem. Rev.* **2006**, *250*, 155.
3. a) Shapiro P. J.: *Coord. Chem. Rev.* **2002**, *231*, 67; b) Prashar S., Antinolo A., Otero A.: *Coord. Chem. Rev.* **2006**, *250*, 133; c) Wang B.: *Coord. Chem. Rev.* **2006**, *250*, 242; d) Antinolo A., Fajardo M., Gómez-Ruiz, S., López-Solera I., Otero A., Prashar S.: *Organometallics* **2004**, *23*, 4062; e) Raith A., Altmann P., Cokoja M., Herrmann W. A., Kühn F. E.: *Coord. Chem. Rev.* **2010**, *254*, 608; f) Gómez-Ruiz S., Prashar S., Fajardo M., Antinolo A., Otero A., Maestro M. A., Volkis V., Eisen M. S., Pastor C. J.: *Polyhedron* **2005**, *24*, 1298.
4. a) Bochmann M.: *Organometallics* **2010**, *29*, 4711; b) Babushkin D. E., Brintzinger H. H.: *J. Am. Chem. Soc.* **2010**, *132*, 452; c) Baldwin S. M., Bercaw J. E., Brintzinger H. H.: *J. Am. Chem. Soc.* **2008**, *130*, 17423; d) Lee L. W. M., Piers W. E., Parvez M., Rettig S. J., Young V. G., Jr.: *Organometallics* **1999**, *18*, 3904.
5. a) Lang H., Seyferth D.: *Organometallics* **1991**, *10*, 347; b) Varga V., Hiller J., Gyepes R., Polášek M., Sedmera P., Thewalt U., Mach K.: *J. Organomet. Chem.* **1997**, *538*, 63;

c) Lukešová L., Gyepes R., Varga V., Pinkas J., Horáček M., Kubišta J., Mach K.: *Collect. Czech. Chem. Commun.* **2006**, *71*, 164.
6. Luinstra G. A., Teuben J. H.: *J. Chem. Soc., Chem. Commun.* **1990**, 1470.
7. a) Erker G., Mollenkopf C., Grehl M., Fröhlich R., Krüger C., Noe R., Riedel M.: *Organometallics* **1994**, *13*, 1950; b) Jödicke T., Menges F., Kehr G., Erker G., Höweler U., Fröhlich R.: *Eur. J. Inorg. Chem.* **2001**, 2097; c) Röll W., Zsolnai L., Huttner G., Brintzinger H. H.: *J. Organomet. Chem.* **1987**, *322*, 65.
8. a) Erker G., Kehr G., Fröhlich R.: *J. Organomet. Chem.* **2004**, *689*, 1402; b) Nie W.-L., Erker G., Kehr G., Fröhlich R.: *Angew. Chem., Int. Ed.* **2004**, *43*, 310; c) Hüerländer N., Kleigrewe N., Kehr G., Erker G., Fröhlich R.: *Eur. J. Inorg. Chem.* **2002**, 2633; d) Knüppel S., Erker G., Fröhlich R.: *Angew. Chem., Int. Ed.* **1999**, *38*, 1923; e) Bai S.-D., Wei X.-H., Guo J.-P., Liu D.-S., Zhou Z.-Y.: *Angew. Chem., Int. Ed.* **1999**, *38*, 1926.
9. a) Horáček M., Štěpnička P., Gyepes R., Císařová I., Tišlerová I., Zemánek J., Kubišta J., Mach K.: *Chem. Eur. J.* **2000**, *6*, 2397; b) Waren T. H., Erker G., Fröhlich R., Wibbeling B.: *Organometallics* **2000**, *19*, 127; c) Lukešová L., Štěpnička P., Fejfarová K., Gyepes R., Císařová I., Horáček M., Kubišta J., Mach K.: *Organometallics* **2002**, *21*, 2639; d) Licht A. I., Alt H. G.: *J. Organomet. Chem.* **2002**, *648*, 134.
10. Horáček M., Pinkas J., Gyepes R., Kubišta J., Mach K.: *Organometallics* **2008**, *27*, 2635.
11. Horáček M., Štěpnička P., Kubišta J., Fejfarová K., Gyepes R., Mach K.: *Organometallics* **2003**, *22*, 861.
12. Horáček M., Gyepes R., Císařová I., Polášek M., Varga V., Mach K.: *Collect. Czech. Chem. Commun.* **1996**, *61*, 1307.
13. Polášek M., Kubišta J.: *J. Organomet. Chem.* **2007**, *692*, 4073.
14. Kriegsmann H., Beyer H.: *Z. Anorg. Allg. Chem.* **1961**, *311*, 180.
15. Varga V., Mach K., Polášek M., Sedmera P., Hiller J., Thewalt U., Troyanov S. I.: *J. Organomet. Chem.* **1996**, *506*, 241.
16. a) Rosenthal U., Burlakov V. V., Arndt P., Baumann W., Spannenberg A.: *Organometallics* **2003**, *22*, 884; b) Beweries T., Burlakov V. V., Bach M. A., Arndt P., Baumann W., Spannenberg A., Rosenthal U.: *Organometallics* **2007**, *26*, 247.
17. Hiller J., Thewalt U., Polášek M., Petrusová L., Varga V., Sedmera P., Mach K.: *Organometallics* **1996**, *15*, 3752.
18. Horáček M., Pinkas J., Kubišta J., Císařová I., Gyepes R., Štěpnička P.: *Collect. Czech. Chem. Commun.* **2007**, *72*, 679.
19. Mach K.: *Titanocenes and Their Interaction with Unsaturated C–C Bonds* (Trzeciak A. M., Ed.), Vol. 9, p. 141. University of Wroclaw, Wroclaw 2005.
20. Xu S.-S., Deng X.-B., Wang B.-Q., Zhou X.-Z.: *Acta Chim. Sinica* **1997**, *55*, 829.
21. Langmaier J., Samec Z., Varga V., Horáček M., Choukroun R., Mach K.: *J. Organomet. Chem.* **1999**, *584*, 323.
22. Horáček M., Štěpnička P., Kubišta J., Gyepes R., Mach K.: *Organometallics* **2004**, *23*, 3388.
23. a) Varga V., Petrusová L., Čejka J., Mach K.: *J. Organomet. Chem.* **1996**, *509*, 235; b) Horáček M., Císařová I., Čejka J., Karban J., Petrusová L., Mach K.: *J. Organomet. Chem.* **1999**, *577*, 103.
24. For definition of agostic interaction see, e.g. a) Brookhart M., Green M. L. H.: *J. Organomet. Chem.* **1983**, *250*, 395; b) Braga D., Grepioni F., Tedesco E., Biradha K., Desiraju G. R.: *Organometallics* **1997**, *16*, 1846; c) Thakur T. S., Desiraju G. R.: *Chem. Commun.* **2006**, 552.
25. Procopio L. J., Carroll P. J., Berry D. H.: *J. Am. Chem. Soc.* **1994**, *116*, 177.

26. a) Ohff A., Kosse P., Baumann W., Tillack A., Kempe R., Görls H., Burlakov V. V., Rosenthal U.: *J. Am. Chem. Soc.* **1995**, *117*, 10399; b) Peulecke N., Ohff A., Kosse P., Tillack A., Spannenberg A., Kempe R., Baumann W., Burlakov V. V., Rosenthal U.: *Chem. Eur. J.* **1998**, *4*, 1852; c) Lamač M., Spannenberg A., Baumann W., Jiao H., Fischer C., Hansen S., Arndt P., Rosenthal U.: *J. Am. Chem. Soc.* **2010**, *132*, 4369.
27. Antropiusová H., Dosedlová A., Hanuš V., Mach K.: *Transition Met. Chem. (London)* **1981**, *6*, 90.
28. Otwinowski Z., Minor W.: *Methods Enzymol.* **1997**, *276*, 307.
29. Altomare A., Burla M. C., Camalli M., Cascarano G., Giacovazzo C., Guagliardi A., Polidori G.: *J. Appl. Crystallogr.* **1994**, *27*, 435.
30. Sheldrick G. M.: *SHELXL97, Program for Crystal Structure Refinement from Diffraction Data*. University of Göttingen, Göttingen 1997.
31. Spek A. L.: *PLATON, A Multipurpose Crystallographic Tool*. Utrecht University, Utrecht 2007.